RESEARCH PAPER

Structural Performance Evaluation of Triangular Rebar Through FEA-Based Topology Optimisation under Multi-Load Scenarios

Himanshu Singh[1], Dr. Arun Kumar Agarwal[2*]
[1]PhD Scholar, Department of Civil Engineering, Uttaranchal University, Dehradun, India.
Email: erhimanshusingh992@gmail.com
[2]Professor, Department of Civil Engineering, Uttaranchal University, Dehradun, India.
Email: blasterarun@gmail.com
***Corresponding author: Himanshu Singh, PhD Scholar, Department of Civil Engineering, Uttaranchal University, Dehradun, India**
Email: erhimanshusingh992@gmail.com
Received: 25th May, 2026; **Revised:** 6th June, 2026; **Accepted:** 8th June, 2026; **Available Online:** 17th June, 2026

ABSTRACT
Traditional methods of reinforcing structures typically waste a large amount of material; however, there have been very few studies investigating the use of advanced materials and topology optimization for developing hollow triangular reinforcement bars that will perform under various load conditions. The focus of this study is to bridge this gap in research by performing finite element analysis (FEA) and topology optimization to determine the structural behaviour of three different types of triangulated reinforcement bars (i.e., Fe500, CFRP, GFRP and titanium) fabricated using advanced materials. For this study, numerical modelling was carried out using a tensile load of 10 kN, and four different types of reinforced concrete beam models were developed; all beams in this study were subjected to four separate points. To ensure they would all meet the displacement limit of 0.5 mm and be within good factors of safety (FS > 2.0), validation had to be completed against the applicable criteria. The results indicated that topology optimization allowed for approximately a 20–22% reduction in the amount of material used to reinforce the concrete beams. The maximum tensile stresses created by the solid bars were calculated as follows: Fe500 = 128.8 MPa, CFRP = 118.8 MPa, GFRP = 96.07 MPa and titanium = 135.9 MPa. Under combined loading, the maximum stresses produced by the optimized hollow triangulated bars also were calculated; they were as follows: Fe500 = 670.83 MPa, CFRP = 601.78 MPa, GFRP = 381.04 MPa and titanium = 531.08 MPa. In addition, the optimized design provided an annual cost savings of 20%, with estimated annual savings reaching ₹9,60,000 per 1000 m of titanium reinforcement.
Keywords: Triangular Reinforcement Bar, Topology Optimization, Tensile Analysis, Flexural Performance.
How to cite this article: Singh H, Agarwal AK. Structural Performance Evaluation of Triangular Rebar Through FEA-Based Topology Optimisation under Multi-Load Scenarios. Int J Drug Deliv Technol. 2026;16(61s): 498-512. DOI: 10.25258/ijddt.16.61s.55
Source of support: Nil.
Conflict of interest: None.

Introduction

Reinforced concrete (RC) structures are utilized in present day civil engineering because of their high strength, durability, versatility and economical benefit. Concrete provides the members of RC excellent compressive strength, while the reinforcement bars (rebar) are employed to resist tensile forces and to increase structural stability [1]. Conventional reinforcement: These are generally made from solid steel bars, the design of which is based on pre-determined requirements and specifications of safety and serviceability [2]. These design approaches have been shown to be effective, but design assumptions may lead to using excess material [3]. With the cost of building materials increasing and environmental issues becoming prominent when making steel, there is an increased demand for new methods of reinforcement which can reduce material usage without compromising the structural strength [4-6].

In the analysis and design of reinforced concrete structures, the situation has undergone an unprecedented revolution in terms of the significant progress made in computer modelling and "finite elements analysis (FEA)" [7]. FEA allows for an in-depth analysis of the distribution of stress, behavior of deformation, crack propagation and load carrying capacity under different loading conditions [8]. The validity of the FEA methodology has been proven through various studies for the prediction of structural response of RC beams reinforced with traditional steel as well as advanced materials such as "Glass Fiber Reinforced Polymer (GFRP)", "Carbon Fiber Reinforced Polymer (CFRP)" and titanium alloys. The material possesses various beneficial properties such as high strength to weight ratio, corrosion resistance and improved durability, which makes it an attractive material for use as a next generation reinforcement material [9].

Meanwhile, topology optimization is a powerful computational design approach for the design of light-weight and material-efficient structural components. The method is systematic, meaning that it's taken out from the low stress areas while preserving the structural integrity and performance [10-12]. In recent research, topology optimization has been proven to be effective in weight reduction of structures, in material cost and environmental impact reduction. The subject of topology optimization of concrete beams and "Hollow structural members (HSM)" has been studied by several researchers and the results have shown the possibility of significant material saving without affecting the strength and stiffness of the members. Most of these studies have been on the improvement of beam geometry and not reinforcement bar configurations [13].

The geometry of the reinforcement bars has a strong influence on bond and stress transfer, crack control and structural behavior of reinforced concrete. There is an increasing amount of practice using circular reinforcement bars, but fewer opportunities to consider non-circular reinforcement geometries [14]. Of these options, triangular reinforcement bars offer some potential advantages, such as increased mechanical interlock with the concrete, improved stress distribution and better suit for topology optimization. Although there are these possible benefits, there is limited research that has explored the structural performance of triangular reinforcement bars with the application of topology optimization and advanced reinforcement materials [15].

This study is motivated by the need for renewable and economical construction materials in the times of increasing demand for them [16]. A decrease in reinforcement material used in building maintenance and strengthening can contribute to a reduction in building costs, carbon footprint and improved resource utilization. Furthermore, insufficient studies on the relative strengths of hollow triangular reinforcement bars with various materials (titanium, carbon fiber, glass fiber and Fe500 steel) under various loads are still lacking [17].

The novelty of the present research is that the optimization and analysis of hollow triangular reinforcement bars by multiple reinforcement materials are realized by combining the finite element analysis and topology optimization. The present study intends to explore the combined effect of reinforcement geometry, material and loading conditions on the performance of the structure, in contrast to the previous studies that primarily studied the effect of traditional reinforcement. This research aims to study the point loading, "uniformly distributed loading (UDL)", "variable linear loading (VLL)" and combined loading condition of a solid and optimized hollow triangular reinforcement in order to find the optimal reinforcement configuration. As such, the specific objectives of this research are:

To numerically evaluate the tensile and flexural performance of solid triangular reinforcement bars fabricated from titanium, carbon fiber, glass fiber, and Fe500 steel.

To develop topology-optimized hollow triangular reinforcement geometries aimed at reducing material consumption while maintaining acceptable displacement and stress limits.

To compare the structural behavior, load-carrying capacity, deformation response, and material efficiency of optimized hollow and conventional solid triangular reinforcement systems under different loading conditions.

To identify the most suitable reinforcement material and optimized geometry based on structural performance and economic considerations.

From the outcome of this study the following outcomes are expected: The optimized configuration of the hollow triangular reinforcement that can reduce the amount of reinforcement materials used while maintaining structural capacity of the reinforced concrete structure; The most efficient reinforcement material among the reinforcement material selected; Design recommendations to incorporate sustainable and lightweight reinforcement system in reinforced concrete structure. The results are expected to help advance next generation reinforcement systems that will help maintain structural performance and environmental sustainability.

Research Methodology

This study involved developing a "finite element analysis (FEA)" and topology optimization methodology to study the use of triangular reinforcement bars made out of Fe500 steel, CFRP, GFRP and Titanium. In addition to conducting solid and hollow (optimized) tensile tests with a 10 kN axial loading. Reinforced concrete beams will also be evaluated under various forms of loading, including point loads, "uniform distributed loads (UDL)", varying linear, and combined loading conditions.

Geometric Modeling of Triangular Reinforcement Bar

The geometric prototype of the triangular reinforcement bar was created using SolidWorks to conduct finite element analysis so that the tensile and flexural performance could be studied. The overall length of the reinforcement bar is 450 mm long and uses an equilateral triangular cross-section with a 20 mm side length. The triangular geometry was selected due to its ability to distribute stresses evenly than a round geometry and offer superior opportunities for topology optimization. The cross-

sectional area of the triangular reinforcement bar was calculated with the following standard geometric equation:

$$A = \frac{\sqrt{3}}{4}a^2 \quad (1)$$

where (A) is the cross-sectional area (mm²) and (a) is the side length of the equilateral triangle (mm). Substituting (a=20) mm gives:

$$A = \frac{\sqrt{3}}{4}(20)^2 = 173.2mm^2$$

This geometry will serve as the reference/starting point for future studies regarding the use and performance of reinforcing bars using FEA, tensile testing and topology optimization.

Material Characterization

A numerical study analysed four types of reinforcing materials (Fe500 Steel, CFRP, GFRP, and Titanium) to represent both traditional metallic materials and modern high strength lightweight composite alternatives. In addition to determining the Young's Modulus, density, Poisson's Ratios; the ultimate tensile and yield strength, which define the stiffness, deformation behaviour, load carrying capability and failure characteristics of the reinforcing bars, were assigned to each type of material [18]. These material properties were used to create a finite element analysis (FEA) model based on established engineering principles and previously validated literature, to ensure the results of the analysis will be accurate and reliable for both tensile and flexural loading [19].

Finite Element Tensile Analysis

Use of SolidWorks Simulation to evaluate the tensile performance of solid triangular reinforcement bars was evaluated using tensile loads of 10 kN along the length of the tube. The end opposing the load was constrained to simulate the axial tensile loading condition [20]. The analytical goals of the analysis were to characterize the distribution of stress, deformation behaviour, and structural performance of various reinforcement materials. The normal tensile stress was established using equations that relate stress to load and linearly distributes over an area:

$$\sigma = \frac{P}{A} \quad (2)$$

where (σ) is the tensile stress (MPa), (P) is the applied tensile load (N), and (A) is the cross-sectional area (mm²). The corresponding tensile strain was determined as:

$$\varepsilon = \frac{\Delta L}{L} \quad (3)$$

where (ΔL) represents elongation and (L) denotes the original length of the bar. The elastic deformation behavior follows Hooke's Law:

$$\sigma = E\varepsilon \quad (4)$$

where (E) is the Young's modulus of the reinforcement material. The relationships noted above were used to evaluate the comparative tensile performance of triangular reinforcement bars.

Topology Optimization of Triangular Rebar

Topology optimization was executed to create an optimal form of a triangular reinforcement bar (the goal was to achieve minimal material use) under axial tensile loading whilst still providing adequate structural performance [21-23]. SolidWorks Simulation provided the means for topology optimization by considering areas of the bar where low levels of stress existed, allowing the removal of those regions without significantly impacting the axial loading capacity of the reinforcement bar. The final outcome of the topology optimization was to reduce the amount of structural material used:

$$Minimize\ M \quad (5)$$

subject to the constraints:

$$\delta_{max} \leq 0.5\text{mm} \quad (6)$$

$$\text{FOS} \geq 2.0 \quad (7)$$

where (M) represents the structural mass, (δ_{max}) is the maximum displacement, and (FOS) denotes the factor of safety. Approximately 20% material reduction on triangular hollow reinforcement was desired for optimized use of materials and to optimise the performance of the triangular hollow reinforcement bar.

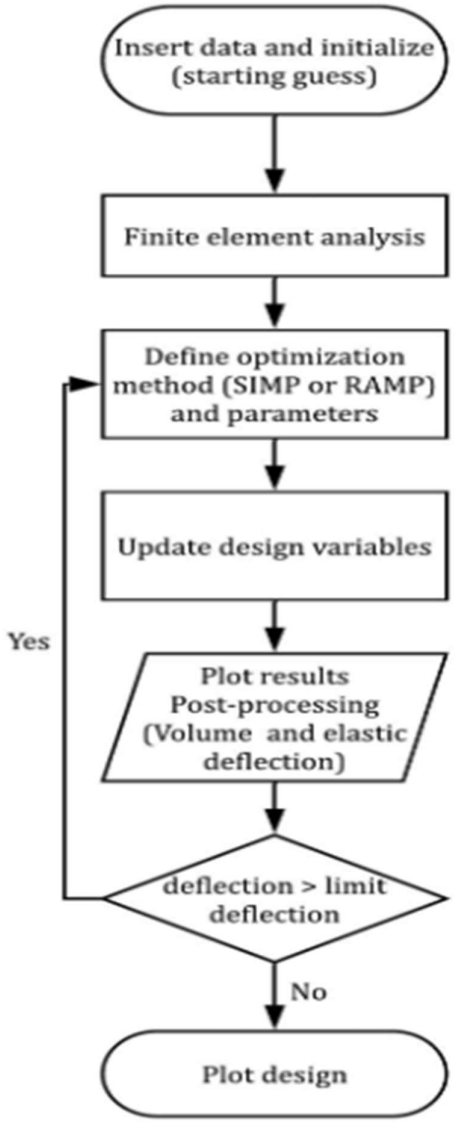

Figure 2: Topology optimization workflow for finite element-based design

Development of Hollow Triangular Reinforcement Bar

The optimized hollow triangular reinforcement bar was created on the basis of results from the topology optimization study, which looked at achieving the most efficient usage of materials while maintaining its structural integrity [24]. The optimized shape still had the traditional triangular shape of equal to 20mm on each side and a total length of 450mm. An additional feature was added to the bar by including the central circular hollow (diameter = 8mm) which acts to decrease the amount of unneeded materials in the areas of lowest stress [25]. The amount of material that was removed due to introducing the hollow core was assessed using the following Material Reduction Percentage:

$$\mathrm{MR}(\%) = \frac{M_s - M_h}{M_s} \quad (8)$$

where (M_s) is the mass of the solid reinforcement bar and (M_h) is the mass of the optimized hollow reinforcement bar. This new bar was used to examine the tensile and flexural behaviour.

Reinforced Concrete Beam Modeling

To evaluate the flexural performance of traditional solid bars and optimal sette hollow triangular reinforcement bars under various loading conditions, a reinforced concrete beam was built using ANSYS Workbench [26]. The beam had a total length of 1500mm, a width of 150mm, a depth of 200mm, and was effectively spanned 1300mm between supports. Due to the extensive nature of M30 concrete in structural applications, that is why M30 concrete was chosen for this application. The bars were installed in the tension zone of the beam, and were provided with a concrete cover of 25mm, to ensure proper bonding between bar and concrete, and also to enable for long-term durability [27-29].

Loading Conditions

Point Load

A concentrated load of 100 kN was applied at the midpoint of a reinforced concrete beam to simulate three point bending, creating a maximum bending moment at the midpoint. Calculation of the maximum bending moment for a three-point loading application can be determined as follows:

$$\mathrm{M} = \frac{PL}{4} \quad (9)$$

where (P) is the applied point load (kN) and (L) is the beam span (mm).

3Uniformly Distributed Load (UDL)

A uniformly distributed load (UDL) of 10 kN/m was applied over the whole span of the reinforced concrete beam to simulate service load conditions typically experienced by structural members, thus creating a uniform bending load across the whole span [30]. The maximum bending moment produced by this loading, under simple supports, can be determined by the following:

$$\mathrm{M} = \frac{wL^2}{8} \quad (10)$$

where (w) is the uniformly distributed load (kN/m) and (L) is the beam span (m).

Varying Linear Load

A triangularly shaped UDL with a maximum intensity of 20 kN/m acting along the entire beam length was applied to simulate the practical application of changing load intensity along the length of the beam. The resultant load is given as:

$$\mathrm{W} = \frac{wL}{2} \quad (11)$$

The corresponding maximum bending moment is:

$$M = \frac{wL^3}{9\sqrt{3}} \quad (12)$$

where (w) is the maximum load intensity and (L) is the beam span.

Combined Loading

The amount of combined loading on a member will create practical applications that normally do not exist, thus simulating the ultimate effect on the total bending moment produced by each load working together, as follows: 1. 100 kN concentrated load, 2. 10 kN/m UDL, and 3. A linear changing load from 0-20kN/m (triangular distributed load). The total bending response will be evaluated using the combined effect of each load acting simultaneously:

$$M_{total} = M_{point} + M_{UDL} + M_{Varying} \quad (13)$$

Evaluation of both hollow and solid normal reinforcement systems.

Performance Evaluation Parameters

The structural performance of both solid and optimized hollow reinforcement systems was evaluated using: Factor of Safety

$$\text{FOS} = \frac{\sigma_{Yield}}{\sigma_{working}} \quad (14)$$

Material Saving

$$MS(\%) = \frac{W_s - W_h}{W_s} \times 100 \quad (15)$$

Cost Saving

$$CS(\%) = \frac{C_s - C_h}{C_s} \times 100 \quad (16)$$

Result and Analysis

The analyses presented determined that topology optimisation yielded a 20 to 22 per cent reduction in reinforcement material while still attaining the desired level of safety. Notably, hollow bars displayed a stress increase ranging from 4.43 to 66.44 per cent. The maximum stress level was attained under combined loading conditions (670.83 MPa for hollow Fe500 reinforcement), whereas the GFRP provided the lowest stress value overall.

3.1 Geometry of Triangular Reinforcement Bar

Figure 3 displays the geometric shape of the solid triangular reinforcement bar used in finite element analysis. Its cross-section is an equilateral triangle (20 mm side and 17.32 mm height) yielding an approximate cross-sectional area of 173.2 mm² as indicated below. Overall, the length of the reinforcement bar is just over 450 mm, providing a slender design. Its uniform triangular shape enables uniform distribution of stress across the entire length of the bar and improves the mechanical interlocking with neighbouring materials. The dimensions of this configuration represent the baseline geometries to be used in the topology optimisation and for evaluating the different structural behaviour under the various loading conditions described above.

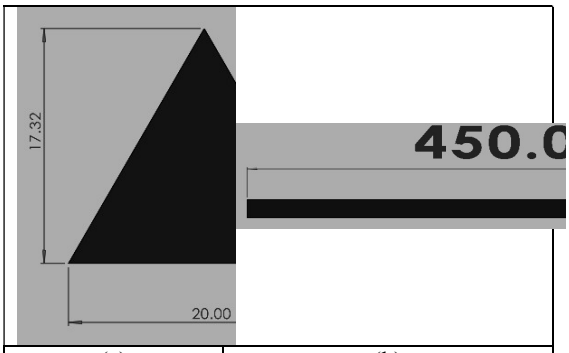

(a) (b)

Figure 3: Geometry of triangular reinforcement bar showing equilateral cross-section with 20 mm side length

3.2. Material Properties

The mechanical characteristics of four kinds of reinforcements for numerical evaluation are shown in Table 1. The elastic modulus values are Fe500 steel (2 × 1011 Pa), CFRP (1.5 × 1011 Pa), titanium (1.1 × 1011 Pa), and GFRP (5 × 1010 Pa), with Fe500 steel being more stiff than all the other materials. CFRP has the highest ultimate microscopic tensile strength (1.8 × 109 Pa), making it the strongest material under tensile loads. The density of the materials listed, in order of heaviest to lightest, is Fe500 steel (7850 kg/m3), CFRP (1600 kg/m3), titanium, and GFRP, with the combination of titanium's higher strength and moderate density and GFRP being lower in stiffness and providing good resistance to corrosion, both being suited for use in lightweight reinforcement applications.

Table 1: Material Parameters used for analysis

Material	Fe500 Rebar	Carbon Fiber Rebar	Glass Fiber Rebar	Titanium Rebar
Elastic Modulus, $E\ (Pa)$	2×10^{11}	1.5×10^{11}	5×10^{10}	1.10×10^{11}
Poisson's Ratio, ν	0.30	0.25	0.25	0.34
Shear Modulus, $G\ (Pa)$	7.9×10^{10}	6×10^{10}	2×10^{10}	4.1×10^{10}
Density $(kg/m3)$	7850	1600	2000	4430
Ultimate Tensile Strength (Pa)	5.45×10^{8}	1.80×10^{9}	1.00×10^{9}	9.50×10^{8}
Yield Strength (Pa)	5.00×10^{8}	No yield (brittle)	No yield (brittle)	8.80×10^{8}

3.3. Static Tensile Analysis of Conventional rock-solid Triangular Rebar

The finite element stress distribution of solid triangular reinforcement bars subjected to a 10 kN tensile force is given in Figure 4. The maximum VMS for each of the materials tested, Fe500 steel (128.8 MPa), CFRP (118.8 MPa), GFRP (96.07 MPa), and titanium (135.9 MPa), indicate a higher stress concentration in titanium than the other materials and less than GFRP. All stresses tested are significantly less than any yield or ultimate strength for the material tested, indicating that the structures tested will perform safely. From the stress contours, the stress distribution along the length of the bar is uniform, with localized concentrations of stress occurring near the edge of the restrained support.

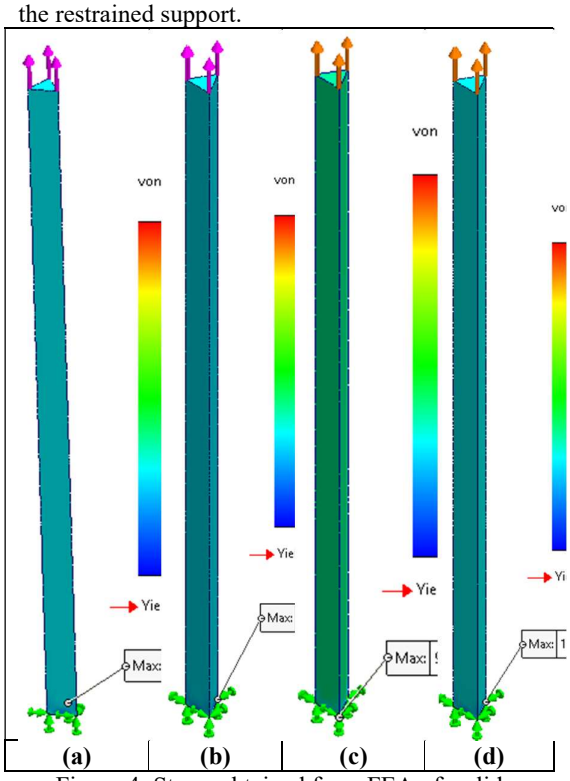

Figure 4: Stress obtained from FEA of solid triangular reinforcement bars under tensile load: (a) Fe500, (b) Carbon Fiber, (c) Glass fiber, (d) Titanium

3.4. Topology Optimization of Triangular Reinforcement Bar

In Table 2, the design parameters that are being used for the topology optimization of the triangular reinforcement bar are summarized. The main aim is to reduce the structural mass while achieving adequate mechanical performance. The target mass is equal to 80% of the original geometry, which corresponds to a 20% reduction in material use. The maximum allowable displacement of 0.5 mm and minimum factor of safety of 2.0 were placed on the design optimization for structural reliability. The optimization was conducted with a consistent tensile load of 10 kN applied throughout. In addition, a symmetry requirement with respect to the longitudinal axis was enforced as a manufacturing constraint so that a practical, balanced, and structurally efficient hollow reinforcement configuration would be achieved.

Table 2. Design goals and objectives for optimization

Parameter	Description
Design Goal	Minimize mass
Target Mass	80% of original mass (20% material reduction)
Constraint 1	Maximum displacement ≤ 0.5 mm
Constraint 2	Factor of safety ≥ 2.0
Load Case	Tensile load of 10 kN
Manufacturing Control	Symmetry about longitudinal axis

Topology optimization results for triangular reinforcement bars subjected to a 10 kN tensile load are shown in Figure 5. The color contours show the areas that must be retained for structural integrity and the areas where material can be removed. The optimization shows that, based on a maximum allowable displacement of 0.5 mm and a minimum factor of safety of 2.0, approximately 20–22% of the material of the centre portion of each reinforcement bar can be removed without violating either of these constraints. The material retained is primarily located in the loading and support areas where the transfer of stress is greatest. The results support the ability to produce hollow triangular reinforcement bars with reduced weight.

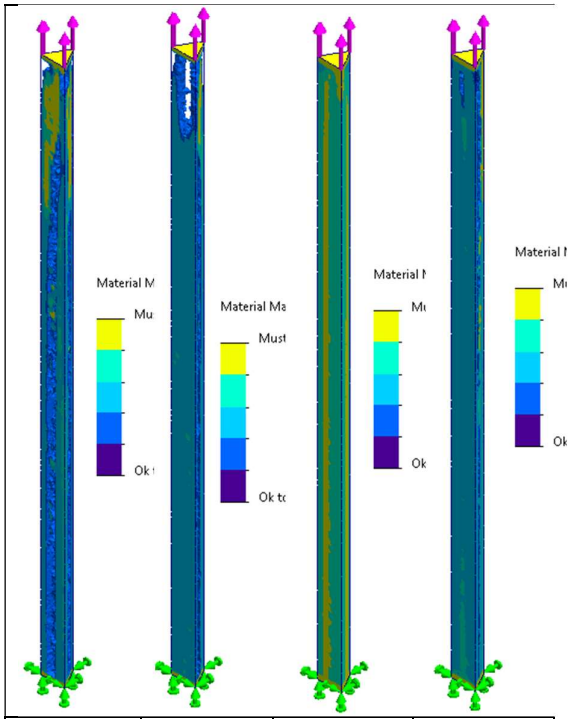

Figure 5: Material distribution obtained from topology optimization analysis, highlighting regions with minimal stress contribution that can be eliminated without significantly affecting structure performance: (a) Fe500, (b) Carbon Fiber, (c) Glass Fiber, (d) Titanium

3.5. Topology-Optimized Hollow Triangular Reinforcement Bar Design

Figure 6 shows the final shape of the topology-optimized hollow triangular reinforcement bar (reinforcement), which was designed following the reduction in material. The optimized section, in addition to containing a centrally located circular hollow core of 8 mm in diameter, contains the same sized equilateral triangular profile (20 mm in side length and 17.32 mm in height) as the original bar. The total length of the bar (450 mm) was kept the same to retain the original design's geometrical compatibility with the standard bar design. Approximately 20-22 percent of the material was saved by using a hollow configuration instead of a solid triangular bar.

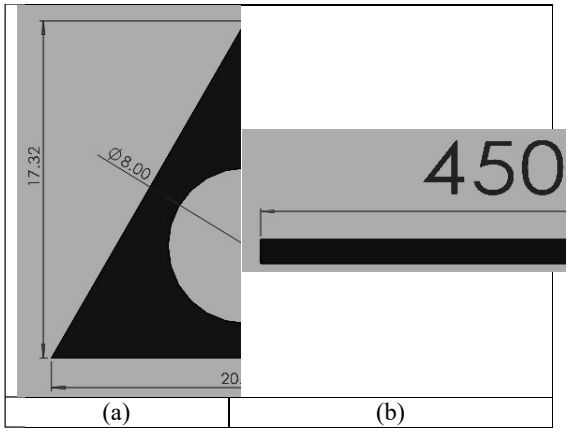

Figure 6: Optimized hollow triangular reinforcement bar geometry: (a)Cross-sectional view showing hollow core, (b) Longitudinal section

3.6. Tensile Behaviour of the Topology-Optimized Hollow Triangular Rebar

Table 3 shows the tensile properties of each of the topology-optimized hollow triangular reinforcement bars that were fabricated from four different base materials. For maximum stress, titanium had the highest result of 181.9 MPa; next was GFRP (159.9 MPa); followed by Fe500 (134.5 MPa); and lastly CFRP (126.2 MPa). The lowest amount of deformation occurred when using Fe500, which had a deformation value of 0.183 mm, indicating the highest stiffness among the four specimens, while GFRP had the largest deformation value of 0.732 mm due to its lower elastic modulus. With an FOS of 14, CFRP had the highest factor of safety and demonstrated the best ability to withstand failure. All materials tested had FOS values greater than or equal to 2.0, demonstrating that all of the topology-optimized hollow reinforcement bars met structural safety requirements.

Table 3: Evaluated parameters of optimized triangular rebar

Property	Fe500	Carbon Fiber	Glass Fiber	Titanium
Maximum Stress induced (MPa)	134.5	126.2	159.9	181.9
Total deformation (mm)	0.183	0.244	0.732	0.332
FOS	3.7	14	6.3	4.8

The distribution of von Mises stresses in hollow triangular reinforcement bars that have been optimised for topology and subjected to a tensile load of 10 kN is shown in figure 7. The maximum calculated stresses for the four different materials:

Fe500, CFRP, GFRP and Titanium are equal to 134.5 MPa, 126.2 MPa, 159.9 MPa and 181.9 MPa respectively. The highest concentration of stress is located at the Titanium followed by GFRP and finally by CFRP as the lowest value of stress amongst the four materials measured. Notwithstanding the fact that there is a hollow core in these elements, all stresses induced are substantially lower than the ultimate or yield strength of the material being studied. High levels of stress concentration are present in the vicinity of the fixed support region.\.

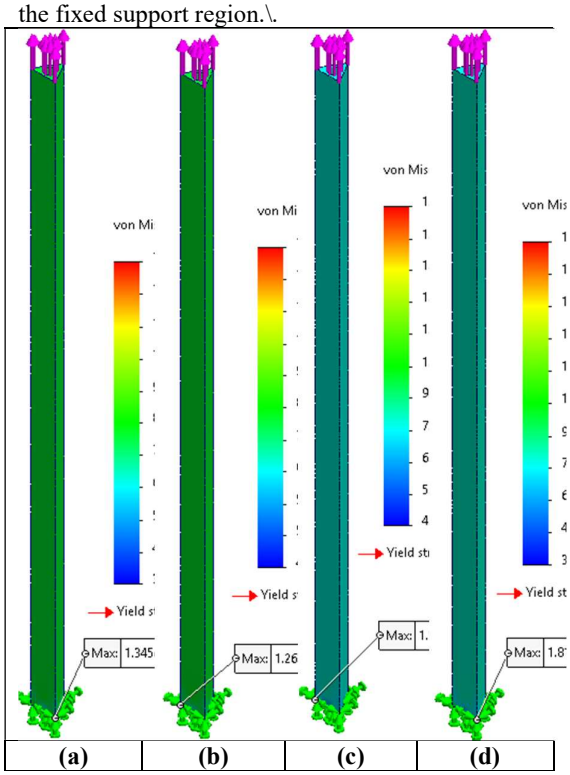

Figure 7: FEA stress allotment in optimized hollow triangular rebar subjected to tensile loading conditions: (a) Fe500, (b) Carbon Fiber, (c) Glass Fiber, (d) Titanium

3.7. Flexural Behaviour of Reinforced Concrete Beams

The four conditions that were used to analyse the four different loading scenarios which were applied during the evaluation of the flexural behaviour of reinforced concrete beams that had triangular rebars were identified in table 4. The loading conditions are described as follows: A concentrated point load (PO) of 100 kN applied at mid span which caused localized bending stresses to occur about that point; 10 kN/m uniform distributed load (UDL) which creates an equivalent load of 65 kN imposed throughout the effective span. The third condition is one whereby the linear loading (varying from zero to 20 kN/m) results in an equivalent load of 48.75 kN with a triangle type distribution. The fourth loading condition consists of a combination of the three different loading types, resulting in an equivalent load of approximately 108.5 kN, which is the most critical and practical service loading effect applied to the structure.

Table 4: Summary of loading conditions for flexural analysis

Condition	Load Type	Magnitude / Distribution	Total Equivalent Load	Location / Application
A	Point Load	100 kN	100 kN	Mid-span
B	Uniformly Distributed Load (UDL)	10 kN/m	65 kN	Entire effective span
C	Varying Linear Load	0 →20kN/m	48.75 kN	Triangular distribution over span
D	Combined Loading	100kN point load + 10kN/m UDL + 0 → 20kN/m varying load	~108.5 kN	Entire span and mid-span

Figure 8 illustrates the loading configuration adopted for flexural analysis under Condition A. A concentrated point load of 100 kN is applied vertically downward at the mid-span of the reinforced concrete beam, simulating a three-point bending test. This loading arrangement produces the maximum bending moment at the beam center, making it suitable for evaluating flexural strength and deformation characteristics. The load is represented as -1.0×10^5 N acting in the negative vertical direction. Under this condition, stress concentration is expected near the loading point and tension zone reinforcement, allowing assessment of crack initiation, load transfer mechanisms, and overall structural response of the beam-reinforcement system.

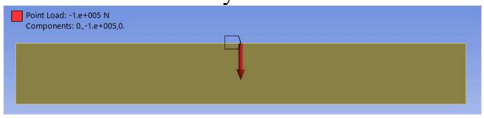

Figure 8: Reinforced concrete beam under mid span concentrated loading

Condition B is defined as the load configuration depicted in Figure 9. A UDL of 10 kN/m is applied vertically downwards for the entire length of the effective span of the reinforced concrete beam for

this loading case. The load is represented as 10,000 N in the finite element model. Due to the nature of a UDL, the applied forces are more uniformly distributed along the beam as opposed to being concentrated at a single point, which causes a more uniform distribution of stresses and reduced stress concentrations throughout the beam. The total load on the beam in this loading case is equivalent to 65 kN. Loading condition B simulates actual service loads that would be experienced on floors and bridge decks, allowing for the evaluation of their flexural capacity, deformation characteristics, and load-carrying capacity.

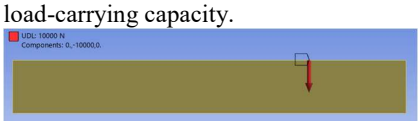

Figure 9: Reinforced concrete beam under uniformly distributed load at full span

The loading condition as shown in Figure 10 is the finite element loading condition (Condition C) having a linearly varying distributed loading applied over the beam span. The linearly varying distributed loading commences with zero kN/m at one end and linearly increases to 20 kN/m at the opposite end resulting in a triangular shaped load distribution. The load distribution is portrayed using a colour scale, which illustrates the range of load intensities for the minimum (blue) and maximum (red) loads on the beam. The total equivalent load produced by this loading distribution is 48.75 kN. The loading condition results in non-uniform bending moment and stress distributions that are created along the beam length due to the distribution of the loads, which allows for evaluating the structural behaviour.

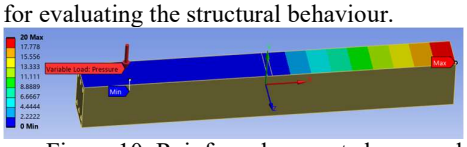

Figure 10: Reinforced concrete beam under uniformly varying load at whole span

Condition D consists of the combined loading condition as displayed in Figure 11. The reinforced concrete beam is loaded simultaneously with a concentrated point load (A) of 100 kN, a uniformly distributed load (B) of 10 kN/m and a linearly varying load ranging from 0 to 20 kN/m (C). The total equivalent load produced by the combination of the three load types is approximately 108.5 kN, which is representative of a realistic service loading condition for a structural application. The loading distribution across the span of the beam produces complex stress and deformation patterns as the result of the load distribution. Therefore, this specific loading condition is anticipated to produce the largest bending moment and stress concentration within the beam and is therefore critical in evaluating the structural performance and stiffness of the beam.

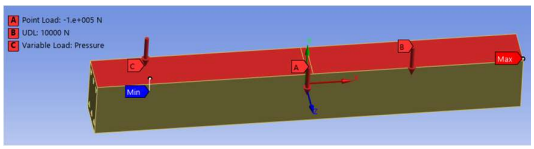

Figure 11: Combined loading at whole span on reinforced concrete beam

The boundary conditions applied to the reinforced concrete beam during finite element analysis are illustrated in Figure 12. The left (B) end acts structurally as a fixed end with no translational movement allowed except vertically, while the right (A) end is modeled as a roller end, allowing horizontal movement to be undertaken but restricting vertical motion. This creates a total beam length of 1,500mm, with 1,300mm of effective span simulating a standard simply supported beam arrangement, widely used within the construction industry. Additionally, the boundary conditions will serve to prevent unrealistic restraint loads and allow for accurate calculations of bending moments, stress distributions, and deformation behaviours of the material.

Figure 12: Fixed supports at span on reinforced concrete beam

Table 5 lists the results of tensile analysis on solid triangular reinforcement bars manufactured from Fe500 steel, CFRP, GFRP, and titanium. The maximum stresses are highest in titanium (135.9 MPa), followed by Fe500 steel at 128.8 MPa (the second highest), CFRP at 118.8 MPa (the third highest) and GFRP at 96.07 MPa (the lowest). The minimum deformation was recorded for Fe500 steel (0.13 mm), which implies that it has the greatest rigidity, whereas GFRP registered the highest deformation value of 0.519 mm (the least rigid, since it has the lowest elastic modulus). All materials satisfy their performance criteria under the applied 10 kN load, with CFRP exhibiting the highest safety factor (15), followed by GFRP (10), titanium (6.5), and Fe500 steel (3.9). All materials demonstrate satisfactory tensile performance from the results obtained.

TABLE 5: Tensile behavior of the solid triangular rebar (Load = 10 KN)

	Fe500 Steel	**CFRP**	**GFRP**	**Titanium**
Maximum Stress induced	128.8	118.8	96.07	135.9

(MPa)				
Total deformation (mm)	0.13	0.173	0.519	0.236
FOS	3.9	15	10	6.5

3.8 Strength Characteristics of Enhanced Hollow Triangular Bars

A comparison was made between the tensile performances of solid vs topology-optimised (hollow) triangular reinforcements using a tensile loading capacity of 10kN. As could be expected, the introduction of the hollow core produces higher levels of stress in all materials due to an overall reduced area of cross-section that is exposed when loaded. Overall, the lowest increase in level of stress after introducing the hollow core was found to be in both Fe500 steel (4.43%) and CFRP (6.23%). This indicates that the performance loss is minimal after optimisation. The overall increase in level of stress found in titanium resulted in a moderate increase (33.85%), whereas GFRP has the highest increase (66.44%) of all four materials with an overall maximum sustained stress of 159.92 MPa. All other materials show there will be an increase in level of deformation. Specifically, after optimization, Fe500 steel increases from 0.13 mm to 0.183 mm, and GFRP increases from 0.519 mm to 0.732 mm. Although these values are increased, all optimised (hollow) rebar will exhibit acceptable structural performance.

TABLE 6: Evaluation of the tensile characteristics between solid and optimized hollow triangular rebar (Load = 10 kN)

Material	**Stress - Solid (MPa)**	**Stress - Hollow (MPa)**	**Stress Increase (%)**	**Deformation - Solid (mm)**	**Deformation- Hollow (mm)**
Fe500 Steel	128.8	134.5	4.43 %	0.13	0.183
CFRP	118.8	126.2	6.23 %	0.173	0.244
GFRP	96.07	159.9	66.44 %	0.519	0.732
Titanium	135.9	181.9	33.85 %	0.236	0.332

Figure 13 provides an illustration of the stress generated within reinforced concrete beams reinforced with solid triangular rebars as a function of four different forms of loading. The maximum recorded stress within the beam under point load conditions by was 145.17 MPa; the minimum stress recorded under uniformly distributed load conditions would be 5.54MPa, due to uniformly distributing load across each of the three spans. The recorded maximum levels of stress for the varying linear load conditions (due to increasing applied load intensity along with the beam) produced maximum levels of stress equal to 439.95 MPa. The combined loading conditions would produce the greatest amount of stress concentration equal to a maximum of 527.47 MPa, and therefore, would have demonstrated the most critical structural response. The largest amount of stress concentration for all possible loading conditions will exist near both support regions and the loaded/axial regions of the beam.

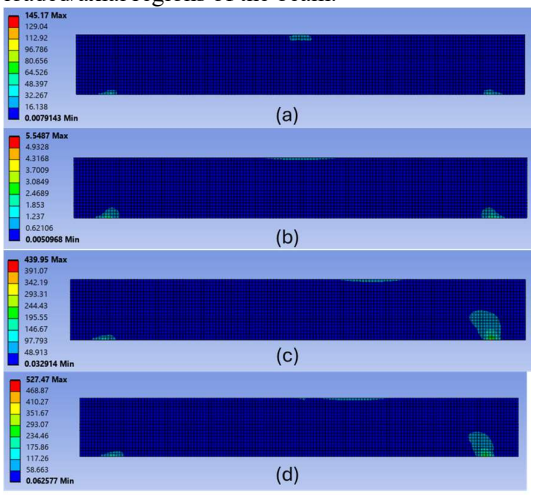

Figure 13: Stress distribution in solid triangular reinforcement Beam: (a) Point load, (b) UDL, (c) Varying load, (d) Combined load

In Figure 14, the stress distribution of reinforced concrete beams with a point load of 100- kN, reinforced with topology optimized hollow triangular bars is demonstrated. The beams exhibit maximum stresses of 151.93 MPa for Fe500 steel, 119.08 MPa for CFRP, 55.73 MPa for GFRP and 92.70 MPa for Titanium. There are higher concentrations of stresses surrounding the loading area of the concrete beams when using Fe500 as compared to the areas of GFRP. The stress contours show that critical stresses are concentrated around the mid-span areas of the beams where concentrated loads are applied. The reduced material was supported by good structural performance and no adverse effect from the variation in topology optimization methods.

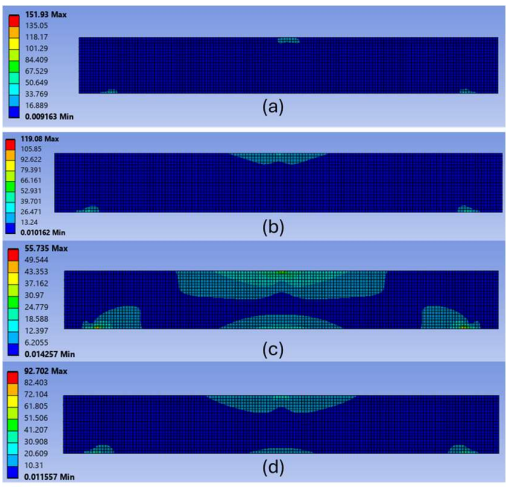

Figure 14: Stress pattern developed within the optimized hollow triangularBeam configuration under point load: (a) Fe500, (b) Carbon Fiber, (c) Glass Fiber, (d) Titanium

As shown in Figure 15, the stresses on reinforced concrete beams are at their greatest levels for point and combined loads of 1-kN/m when compared with uniformly distributed loads of 100-kN. For this reason, the maximum stress levels obtained from a uniformly distributed loading of 10 kN/m are 6.03 MPa for Fe500 steel, 4.83 MPa for CFRP, 3.35 MPa for GFRP and 3.72 MPa for Titanium. Again, the maximum stress is concentrated around the support regions of beams reinforced with Fe500 and the lowest stress is around the support of beams reinforced with GFRP. Due to the fact that the load is uniformly distributed over the entire length of the beam with only one loading point as compared to other loading conditions, the stress level on the concrete and the steel member is lower. Further, the stress contour shows a general uniform distribution with localized areas of increased stress around the support of the beam where the load is being applied.

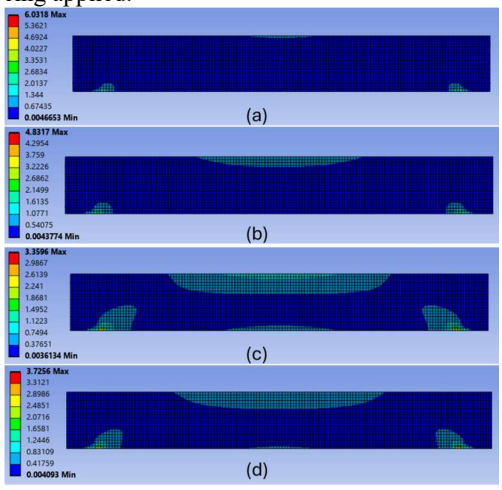

Figure 15: Stress distribution in optimized hollow triangular reinforced concrete beams under uniformly distributed load (UDL): (a) Fe500 steel, (b) CFRP, (c) GFRP, and (d) Titanium.

The stress contour for a reinforced concrete beam supported by topology optimized hollow triangular bars, with varying linear loads (0 kN/m - 20 kN/m), is shown in figure 16.

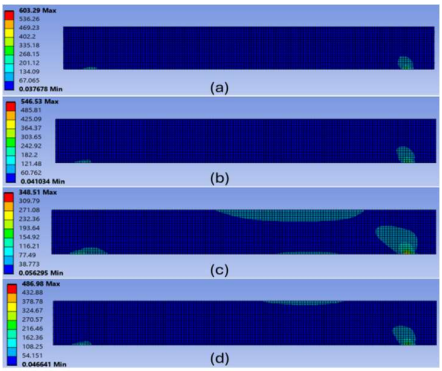

Figure 16: Stress patterns in optimized hollow triangular beams change withVarying load: (a) Fe500, (b) Carbon Fiber, (c) Glass Fiber, (d) Titanium

The maximum stresses found in the beam with Fe500 steel, CFRP, GFRP and Titanium were 603.29 MPa, 546.53 MPa, 348.51 MPa and 486.98 MPa respectively. The Fe500 steel bar induced the highest stress concentration, while the GFRP bar created the lowest. The design of non-uniformly distributed loads will produce non-uniformly distributed stress in the beam. Consequently, the largest stress concentrations occur within the heavily loaded areas of the beam span and at the points where the beam is supported, demonstrating the large impact of asymmetrical loading on the flexural performance of the beam.

Loaded combined with applied point load (100 kN), uniform distributed load (10 kN/m) and varying distributed load (0 kN/m - 20 kN/m) will have the greatest impact on the stresses .created within the concrete beam while being reinforced using topology optimized hollow triangular bars. The maximum stresses generated is shown in figure 17 within the beam using Fe500 steel, CFRP, GFRP and Titanium were 670.83 MPa, 601.78 MPa, 381.04 MPa, and 531.08 MPa, respectively. The Fe500 steel bar produced the greatest stress concentration, while the GFRP bar had the lowest stress concentration. Using combined loading conditions created the greatest structural response for all loading conditions, resulting in the highest stress concentrations located at critical loading points between supports and at the points of support for the concrete beam, which establishes the conditions for the overall governing design.

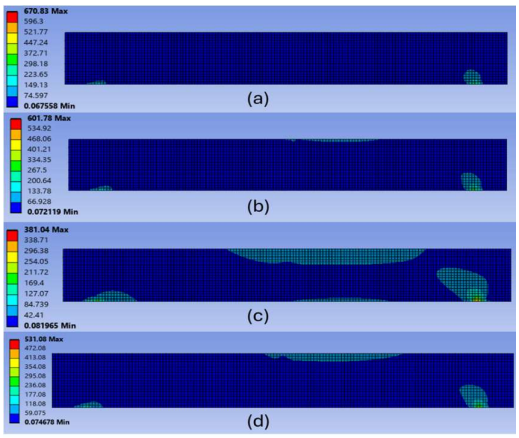

Figure 17: Stress pattern in the optimized hollow triangularBeam change with undercombined load: (a) Fe500, (b) Carbon Fiber, (c) Glass Fiber, (d) Titanium

Table 7 shows the maximum stress and deformation responses of reinforced concrete beams in four different loading conditions. As presented in the first condition of point loading, the hollow Fe500 bar with optimum density has a maximum stress of 151.93 MPa and a maximum deformation of 1.07 mm, which is slightly greater than that of the solid Fe500 bar (145.17 MPa & 1.00 mm). The least amount of stress came with the UDL condition (spanning from a maximum of 3.35 MPa to a maximum of 6.03 MPa for deformation) and no deformation of any of the beams that had UDLs has exceeded 0.06 mm. For the varying linear load condition, the stress ranged up to 603.29 MPa (the maximum attained with the hollow Fe500). The maximum deformation for the varying linear load on both the combined loading condition and the GFRP were 670.83 MPa and 5.41 mm respectively.

Table 7: Shows the results of the analysis when we use different loads conditions

Loading Condition	Reinforcement Type	Max Stress (MPa)	Max Deformation (mm)
Condition A: Point Load (100 kN)	Solid Bar (Fe500)	145.17	1.00
	Optimized Hollow Bar (Fe500)	151.93	1.07
	Optimized Hollow Bar (CFRP)	119.08	1.12
	Optimized Hollow Bar (GFRP)	55.73	1.27
	Optimized Hollow Bar (Titanium)	92.70	1.17
Condition B: UDL (10 kN/m)	Solid Bar (Fe500)	5.54	0.04
	Optimized Hollow Bar (Fe500)	6.03	0.05
	Optimized Hollow Bar (CFRP)	4.83	0.05
	Optimized Hollow Bar (GFRP)	3.35	0.06
	Optimized Hollow Bar (Titanium)	3.72	0.05
Condition C: Varying Linear Load (0→20kN/m)	Solid Bar (Fe500)	439.95	3.36
	Optimized Hollow Bar (Fe500)	603.29	3.58
	Optimized Hollow Bar (CFRP)	546.53	3.77
	Optimized Hollow Bar (GFRP)	348.51	4.24
	Optimized Hollow Bar (Titanium)	486.98	3.93
Condition D: Combined Loading	Solid Bar (Fe500)	527.47	4.27
	Optimized Hollow Bar (Fe500)	670.83	4.56
	Optimized Hollow Bar (CFRP)	601.78	4.80
	Optimized Hollow Bar (GFRP)	381.04	5.41
	Optimized Hollow Bar (Titanium)	531.08	5.01

Figure 18 compares the maximum stress developed in reinforced concrete beams from the four different loading conditions, using both solid and topology-optimized hollow reinforcement bars. Under the 2nd loading condition of UDL, the maximum stress observed was between 3.35 MPa and 6.03 MPa. Under the 1st loading condition of point load, the maximum stress developed by either solid or hollow bars was in the range of 55.73 MPa to 151.93 MPa. Under loading condition 3 (varying linear load), significant increases in maximum stresses were noted, i.e., 603.29 MPa for the hollow

Fe500 bar. Under loading condition 4 (combined loading), the maximum stress developed from the optimized hollow Fe500, CFRP, GFRP and titanium were 670.83 MPa, 601.78 MPa, 381.04 MPa and 531.08 MPa respectively. Overall, GFRP had the least amount of stress developed.

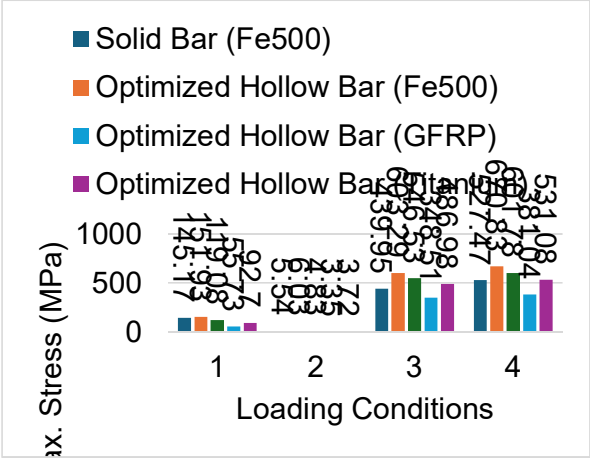

Figure 18: Comparemaximum stress over all loading conditions for each reinforcement material

3.9 Cost Comparison

Topology optimization was used to achieve various economic benefits regarding the use of triangular reinforcement bars. By using a consistent approach to reduce the material by approximately 20%, there are equivalent savings in the cost of the material used for all types of reinforcement. The cost of a Fe500 steel reinforcement bar was reduced from ₹185/m to ₹148/m and will save approximately ₹37,000 each year per 1,000 m. A CFRP reinforcement bar was reduced as well (from ₹2,500/m to ₹2,000/m) and will save approximately ₹5,00,000 each year. A GFRP bar was reduced (from ₹1,200/m to ₹960/m), generating an annual savings of ₹2,40,000. When analyzing the expected savings of Titanium reinforcement bars, it was evident that the most significant economic benefit resulted from a reduction from ₹4,800/ m to ₹3,840/m, which could generate an expected annual savings of ₹9,60,000 (the highest reported). Based on the above results, topology optimization greatly improved the efficiency and cost-effectiveness of the material used while not reducing its structural performance.

TABLE 8: Results of the cost analysis for the triangular reinforcement bars

Material	Cost of Solid Rebar (₹/m)	Cost of Optimized Hollow Rebar (₹/m)	Cost Saving (%)	Estimated Annual Savings (per 1000 m)
Fe500 Steel	₹185/m	₹148/m	20.0 %	₹37,000
CFRP	₹2,500/ m	₹2,000/m	20.0 %	₹5,00,000
GFRP	₹1,200/ m	₹960/m	20.0 %	₹2,40,000
Titanium	₹4,800/ m	₹3,840/m	20.0 %	₹9,60,000

Conclusions

This study evaluated how conventional solid triangular reinforcement bars made of Fe500, CFRP, GFRP, and Titanium with topology optimized hollow cores perform structurally by using finite element analysis and topology optimization methods. The solid triangular reinforcement bars were tested under a 10 kN of tensile load producing maximum stresses of 128.8 MPa for Fe500, 118.8 MPa for CFRP, 96.07 MPa for GFRP, and 135.9 MPa for Titanium. By adding an 8 mm hollow core to each of the aforementioned materials, topology optimization enabled a reduction of approximately 20% –22% of material volume while still producing a maximum displacement of 0.5 mm and having a safety factor greater than 2.0. When comparing the stress results of the optimized hollow triangular reinforcement bars to the solid triangular reinforcement bars, there were 4.43%, 6.23%, 66.44%, and 33.85% respectively increases in Fe500, CFRP, GFRP, and Titanium. The analysis revealed that under a flexural load of combined loading; the structural response will be at its worst, generating maximum stress results of 670.83 MPa for Fe500, 601.78 MPa for CFRP, 381.04 MPa for GFRP and 531.08 MPa for Titanium. The cost analysis showed at least a 20% savings in the cost of reinforcement and produced an annual savings of ₹9,60,000 per 1000 m of Titanium reinforcement. The results of this study indicate that topology optimized hollow triangular reinforcement bars are a cost-effective, efficient, and sustainable alternative to conventional solid reinforcement systems.

References:

O. A. Mohamed and R. Khattab, "Numerical Analysis of Reinforced Concrete Beam Strengthened with CFRP or GFRP Laminates," *Key Engineering Materials* 707 (September 2016): 51–59. https://doi.org/10.4028/www.scientific.net/KEM.707.51.

Yangjun Luo, Michael Yu Wang, Mingdong Zhou, and Zhihao Deng, "Topology Optimization of Reinforced Concrete Structures Considering Control of Shrinkage and Strength Failure," *Computers & Structures* 157 (2015): 31–41. https://doi.org/10.1016/j.compstruc.2015.05.009.

Ijaz Ahmed, Sebastian Reichenbach, and Bernd Kromoser, "Flexural Behaviour of Reinforced Concrete Beams with Voids: Topology

Optimisation Basis," *Structures* 67 (2024): Article 107037. https://doi.org/10.1016/j.istruc.2024.107037.

Y. Shao, T. Zhao, J. Yan, C. P. Ostertag, and G. H. Paulino, "Improving the Ductility of Concrete Beams Reinforced with Topologically Optimized Steel," *Journal of Structural Engineering* 151, no. 4 (2025). https://doi.org/10.1061/JSENDH.STENG-13908.

T. Xue, X. Yuan, and Zhi [Initial Unknown], "Loading Methods Effect on Behavior of RC Beam-Column Sub-Assemblages to Resist Progressive Collapse," *Key Engineering Materials* (2024): 73–80. https://doi.org/10.4028/p-iwujy3.

P. J. Yu and S.-Y. Lee, "Design Applicability and Parametric Simulation of an RC Pier Column Using Hollow Rebars," *Journal of the Korean Society of Advanced Composite Structures* 14, no. 3 (2023): 20–26. https://doi.org/10.11004/KOSACS.2023.14.3.020.

Z. Xu, S. Chen, and Q. Hao, "Analytical Bond Strength of Deformed Bars in Concrete Confined with Transverse Reinforcement and FRP," *Engineering Structures* 280, no. 2 (2023): Article 115594. https://doi.org/10.1016/j.engstruct.2023.115594.

G. B. Sakcalı and İ. Yüksel, "Numerical Simulation of GFRP-Reinforced Rectangular Concrete Beams and Proposed Design Expressions," *PeriodicaPolytechnica Civil Engineering* 69 (2024): 263–279. https://doi.org/10.3311/PPCI.37254.

Oded Amir, "A Topology Optimization Procedure for Reinforced Concrete Structures," *Computers & Structures* 114–115 (2013): 46–58. https://doi.org/10.1016/j.compstruc.2012.10.011.

Abeygunawardana, Navoda, Hikaru Nakamura, Tatsuya Nakashima, and Taito Miura. "Numerical investigation of the effect of straight development length on the anchorage performance of 180-degree rebar hooks." *Infrastructures* 11, no. 3 (2026): 93.

Encalada, Lider S., Emily D. Munoz, Diego A. Sosa, Melisa N. Herrera, Juan C. Velastegui, and Christian M. Gómez. "Seismic performance assessment of risk category III Ecuadorian buildings made of reinforced concrete frames and flat slabs." In *Structures*, vol. 87, p. 111612. Elsevier, 2026.

Shin, Jihun, and Chang-Su Shim. "Mechanical degradation of naturally corroded rebars from a 45-year-old bridge slab: 3D quantification of section loss and a new corrosion damage indicator." *Case Studies in Construction Materials* (2026): e05893.

Apostolou, Fotios. "Seismic performance evaluation of an existing 4-storey reinforced concrete commercial building." (2026).

Huang, Jiaying, Huatian Zhao, Yang Gao, and Gang Shi. "Numerical study on cyclic behaviour of triple grades hybrid high-performance steel structure." *Engineering Structures* 327 (2025): 119605.

Kim, Sangwoo, Wonchang Choi, and Jinsup Kim. "Performance Evaluation of Reinforced Concrete Beams with Corroded Rebar Strengthened by Carbon Fiber-Reinforced Polymer." *Polymers* 17, no. 8 (2025): 1021.

Kim, Tae-Hoon. "Seismic performance assessment of deteriorated two-span reinforced concrete bridges." *International Journal of Concrete Structures and Materials* 16, no. 1 (2022): 4.

Ekolu, S. O., T. Thomas, W. Lawrence, L. De Freitas, I. van Vuuren, and F. Solomon. "Effects of triangular reinforcing on flexural and deformation behaviour of concrete beams." *Journal of Building Pathology and Rehabilitation* 9, no. 2 (2024): 123.

Shi, Gang, Huatian Zhao, and Yang Gao. "Development of triple grades hybrid high-performance steel structure (TGHSS): Concept and experiments." *Engineering Structures* 266 (2022): 114654.

Huang, Yuan, Bing Han, and Wenmeng Yin. "Reinforced concrete corbels shear test: the triangular-truss method evaluation." *Buildings* 12, no. 10 (2022): 1619.

박은상. "Seismic Performance of Reinforced Concrete Columns with Spirals and 700 MPa Longitudinal and Transverse Reinforcing Bars." PhD diss., 서울대학교 대학원, 2024.

Singh, Prakash Abhiram, Yogesh Deoram Patil, and Rahul Tarachand Pardeshi. "Performance evaluation of triangular and circular bulged perforated headed stud shear connector in composite junction." In *Structures*, vol. 53, pp. 327-345. Elsevier, 2023.

Xiao, Shuijing, Guanzheng Zhou, Peng Feng, and Zhe Qu. "Seismic performance evaluation of novel RC frame structure with kinked rebar beams and post-yield hardening columns through shaking table tests." *Engineering Structures* 290 (2023): 116375.

Ekolu, S. O., T. Thomas, W. Lawrence, L. De Freitas, I. van Vuuren, and F. Solomon. "Effects of triangular reinforcing on structural behaviour of concrete beams." (2024).

Koshy, Ms Bency Mariyam, and Mr Jinu Darsh. "Performance Evaluation of Composite Wall with Boundary Column Having Triangular Corrugation."

Navarro, D., R. Valero, and J. Orihuela. "Evaluation of the Influence of Different Grades of Reinforcing Steel on the Seismic Performance of Concrete reinforced Frame Structures with Nonlinear Static Analysis." In *IOP Conference Series: Materials Science and Engineering*, vol. 1048, no. 1, p. 012022. IOP Publishing, 2021.

Raza, Ali, Syyed Adnan Raheel Shah, Hatem Alhazmi, Muhammad Abrar, and Samia Razzaq.

"Strength profile pattern of FRP-reinforced concrete structures: A performance analysis through finite element analysis and empirical modeling technique." *Polymers* 13, no. 8 (2021): 1265.

Luo, Qirui, Wei Wang, Zhuangzhuang Sun, Shanwen Xu, and Bingjie Wang. "Seismic performance analysis of corrugated-steel-plate composite shear wall based on corner failure." *Journal of Constructional Steel Research* 180 (2021): 106606.

Kamde, Deepak K., Karthikeyan Manickam, Radhakrishna G. Pillai, and George Sergi. "Long-term performance of galvanic anodes for the protection of steel reinforced concrete structures." *Journal of Building Engineering* 42 (2021): 103049.

Bakkar, Md Abu, Rajib Saha, and Debdulal Das. "Low cycle fatigue performance and failure analysis of reinforcing bar." *Metals and Materials International* 27, no. 12 (2021): 4952-4966.

Siddiquee, Kader Newaj, AHM Muntasir Billah, and Anas Issa. "Seismic collapse safety and response modification factor of concrete frame buildings reinforced with superelastic shape memory alloy (SMA) rebar." *Journal of Building Engineering* 42 (2021): 102468.